Improved Monte Carlo model for multiple scattering calculations

Weiwei Cai (蔡伟伟) and Lin Ma (马 林)*

Department of Mechanical Engineering, Clemson University, Clemson, SC 29634

**Corresponding author: LinMa@clemson.edu*

Received March 7, 2011; accepted May 14, 2011; posted online August 24, 2011

The coupling between the Monte Carlo (MC) method and geometrical optics to improve accuracy is investigated. The results obtained show improved agreement with previous experimental data, demonstrating that the MC method, when coupled with simple geometrical optics, can simulate multiple scattering with enhanced fidelity.

OCIS codes: 290.4210, 290.4020, 290.7050.

doi: 10.3788/COL201210.012901.

Multiple scattering is a fundamental problem with applications in a wide spectrum of systems. Notable application examples where multiple scattering holds an important role include laser imaging through biological tissues[1], remote sensing in the atmosphere[2], and the development of laser diagnostics for dense sprays[3]. Fundamentally, the multiple scattering problem requires solving the wave equation in a system of a large number of scatterers, which is extremely difficult[4]. Under certain assumptions, the problem can be simplified and the radiative transfer equation (RTE) can be derived[5]. However, the solution of the simplified RTE is also difficult under practical conditions (e.g., anisotropic phase function and non-ideal geometry), therefore there is a need to resort to numerical techniques. The Monte Carlo (MC) method has been demonstrated as a powerful numerical technique for multiple scattering calculations, which is capable of simulating multiple scattering under various configurations and shows good agreement with experiments[6−8]. On the other hand, the limitations of the MC method are also well recognized, and the development of new MC methods continues to be an active area of research. For example, considerable progress has been made in the experimental validation of MC methods[6,7] and in the improvement of their efficiency[9,10]. Meanwhile, new MC methods have been developed to track the polarization during multiple scattering[11,12] and to capture the propagation of an ultra-short laser pulse in optically dense media[13].

Based on previous studies, this letter investigates the coupling between the MC method and geometrical optics. The results obtained using the new model show improved agreement with previous experimental data. Such an improved agreement demonstrates that the MC method, when coupled with simple geometrical optics, can simulate multiple scattering with enhanced fidelity.

Figure 1 illustrates the multiple scattering problem studied in this letter. A collimated laser beam (labeled as the "incident beam") illuminates a cubic cell containing the scattering media. The beam is aligned perpendicular to the incident plane of the cell, whose direction defines the x axis of a Cartesian coordinate as shown in the figure. The origin of the coordinate is defined as the center of the exit plane of the cell, and the y and z axes are defined to be parallel to the edges of the exit plane. The incident photons are scattered multiple times by the media, as illustrated by the zigzag line, and the scattering events are simulated using a MC model. After a certain number of scattering events, the incident photons exit the cell via transmission through the exit plane, reflection through the incident plane, or transmission through the four side planes of the cell. This study considers all three scenarios. For illustration purposes, Fig. 1 shows the transmission of a photon through the exit plane to facilitate the description of our model. The direction of a transmitted photon after the last scattering event (i.e., in the direction of OA) is completely defined by the azimuthal angle (θ) and the zenith angle (ϕ). The scattering angle relative to the x axis (i.e., β) after the last scattering event can be expressed as

$$\cos\beta = \sin\phi \cdot \cos\theta. \tag{1}$$

Due to the refractive index mismatch between the scattering media (water) and the ambience (air), the angle (β') of a transmitted photon after the refraction is determined by the following:

$$n_{\mathrm{w}} \sin\beta = n_{\mathrm{a}} \sin\beta', \tag{2}$$

where β' is the final exit direction of a transmitted photon out of the exit plane, n_{w} is the refractive index of water (taken to be 1.33 in this study), and n_{a} is the refraction index of air (taken to be 1). The refraction changes the azimuthal and the zenith angles of the direction of propagation correspondingly (from θ and ϕ to θ' and ϕ', respectively). The new azimuthal (θ') and the zenith

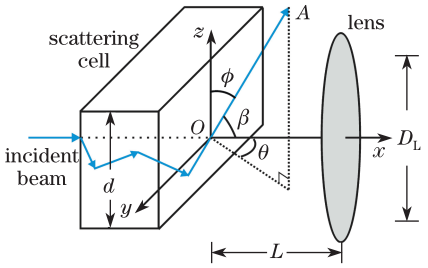

Fig. 1. Illustration of the model configuration and definition of the coordinate system.

angles (ϕ') after refraction are determined by solving the following equations:

$$\cos\beta' = \sin\phi' \cdot \cos\theta' \tag{3}$$

and

$$\frac{\cos\phi'}{\cos\phi} = \frac{\sin\beta'}{\sin\beta}. \tag{4}$$

In order to be transmitted, the scattered photons must travel through the scattering media (which have higher refractive index) into air (which has lower refractive index). Therefore, total reflection can occur and prevent a portion of the photons from transmitting through the exit plane. The critical angle of total reflection is determined by the following equation:

$$\beta_{\rm c} = \sin^{-1}\left(\frac{n_{\rm a}}{n_{\rm w}}\right). \tag{5}$$

Photons that have a scattering angle β larger than $\beta_{\rm c}$ after its last scattering event are scattered back into the media, while those that have a β smaller than $\beta_{\rm c}$ will be partially transmitted and the transmission is given by the following[14]:

$$T = 1 - \frac{1}{2}\left\{\left[\frac{(n_{\rm w}/n_{\rm a})\cos\beta - \cos\beta'}{(n_{\rm w}/n_{\rm a})\cos\beta + \cos\beta'}\right]^2 + \left[\frac{\cos\beta - (n_{\rm w}/n_{\rm a})\cos\beta'}{\cos\beta + (n_{\rm w}/n_{\rm a})\cos\beta'}\right]^2\right\}. \tag{6}$$

Such refraction/reflection effects as described in Eqs. (2)–(6) have been discussed previously[15,16], but they are also often neglected[1,6,7]. Therefore, one goal of this study is to quantitatively examine such effects. Results obtained in this research show that such effects affect both the profile and the magnitude of the distribution of the scattered photons.

In practice, scattered photons are collected by an imaging system. In this study, again using the example of transmission through the exit plane, the imaging system is considered by a lens (whose diameter is $D_{\rm L}$) placed at a distance of L away from the exit plane. At a given $D_{\rm L}$ and L, the determination of whether a transmitted photon can be collected by the lens depends both on the direction of propagation (characterized by θ' and ϕ') and the location of the last scattering event (characterized by $y_{\rm e}$ and $z_{\rm e}$). The following condition must be satisfied for a transmitted photon to be collected by the lens:

$$\sqrt{(y_{\rm e} + L\cdot\tan\theta')^2 + \left(z_{\rm e} + \frac{L}{\cos\theta'\cdot\tan\phi'}\right)^2} \leqslant \frac{D_{\rm L}}{2}. \tag{7}$$

In summary, Eqs. (1)–(7) completely describe the transmission of photons through the exit plane. More specifically, the model used in this study used Eqs. (1)–(3) to calculate the direction of the transmitted photons, Eqs. (5) and (6) to determine the fraction of photons that are transmitted, and Eq. (7) to determine the fraction of transmitted photons that are collected by the lens. Similar equations are developed for photons that exit the cell through other planes and implemented in the model.

Based on the above discussions, a MC model was implemented to simulate multiple scattering in the cell, incorporating Eqs. (1)–(7) to account for reflection, refraction, and collection. The MC model was implemented according to Ref. [8] using FORTRAN90. In the model, photons were generated one by one and sent into the scattering cell, where they performed a random walk in three dimensions. The step length was generated from an exponential distribution determined by the scattering coefficient of the media; the direction of each step was generated from the phase function of the scatterer calculated using the Mie theory[17]. The model determines if each photon exits the cell after each step. Equations (1)–(7) are used to determine the location/direction of the exit and whether it is collected by the imaging system. Otherwise, the random walk continues until the photon exits.

The model described above was applied to simulate multiple scattering in a cell, and the results were compared with experimental data reported in Refs. [6, 18]. We first briefly summarized the experiments performed in Refs. [6, 18] to facilitate the discussion in this study. In previous experiments, a collimated laser beam at a wavelength of $\lambda = 800$ nm was used as the incident beam. The incident beam probed into a quartz cell (d=10 mm), which contained a scattering media consisting of distilled water and polystyrene particles (with diameter D=1, 5, and 10 μm). A chargel-coupled device (CCD) camera was then used to record the distribution of the scattered photons. These experiments used two imaging lenses, both with a focal length of 10 cm, but different sizes ($D_{\rm L}$=5.55 and 1.79 cm, respectively). The lenses were placed at a distance of L=15.2 cm away from the surface to be imaged. Based on the geometry of the lens, an acceptance angle can be defined as

$$\theta_{\rm a} = \tan^{-1}\left[\frac{(D_{\rm L} - d)/2}{L}\right]. \tag{8}$$

The larger lens (with $D_{\rm L} = 5.55$ and $F/\# = 1.8$) corresponds to $\theta_{\rm a}$= 8.5°, while the smaller lens (with $D_{\rm L} =$ 1.79 and $F/\# = 5.6$) corresponds to $\theta_{\rm a}$= 1.5°.

Note that $\theta_{\rm a}$ only serves as a simplified and qualitative indicator of the collection efficiency of the imaging systems. In practice, each transmitted photon exits at a different location; depending on the exit location, a photon exiting at an angle larger than $\theta_{\rm a}$ may still be collected. Therefore, quantitative analysis of the collection requires the use of Eqs. (1)–(7), as implemented in our model.

The parameters in our model were set to match those used in the experiments in order for direct comparisons to be made between the simulations of our model and the experiments. The refractive index of the polystyrene particles was taken to be 1.578. At each particle size, the particle concentration was adjusted to achieve the desired optical depth (OD). The intensity profiles of the incident laser beams used in the model are shown in Fig. 2, which are obtained by measuring the transmitted laser beam at the exit plane with the cell containing distilled water but no polystyrene particles. The intensity profile of the incident laser beams is found to be approximately Gaussian along the z axis, thus this study uses the full-

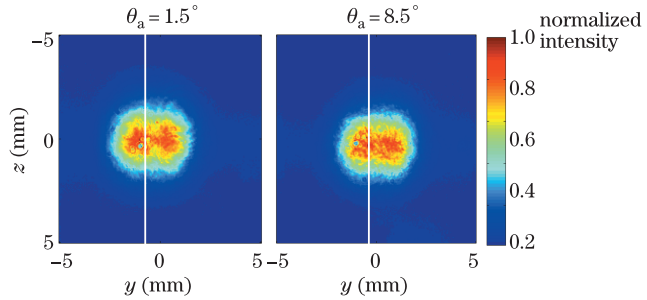

Fig. 2. Intensity distribution of the incident laser beams used in the model.

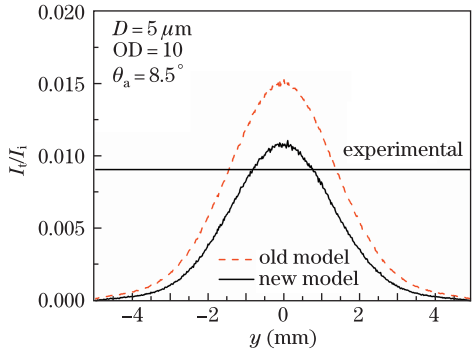

Fig. 3. Intensity profile of the transmitted photons obtained using the new model in comparison to the results obtained from the old model and the experiments.

width at half-maximum (FWHM) to characterize the intensity profile. The FWHM of the incident laser beam was measured to be 2.55 mm at θ_a=8.5° at y=0 and 2.61 mm at θ_a=1.5° at y=0. These intensity profiles were used as the input in the MC model to simulate the intensity profile of the scattering photons.

Figure 3 shows a set of transmission profiles at the exit plane obtained by our model described above (termed as the "new model" hereinafter). The transmission is defined as I_t/I_i, where I_i represents the intensity of the incident laser and I_t the intensity of the transmitted beam. The results obtained by the new model was compared against the results obtained from experimental measurements and from a model that does not consider the refraction, total reflection, and collection by the lens (termed as the "old model" hereinafter). The line showing the experimental result corresponds to the peak transmission, which was measured along the line shown in Fig. 2 (where the maximum transmission occurs).

Comparisons were also made under other conditions, and the results are summarized in Fig. 4. Figure 4(a) compares the maximum transmission, while Fig. 4(b) shows the difference of the model predictions relative to the experimental value. As can be seen from these results, the new model consistently predicts a lower transmission and shows better agreement with the experimental data than the old model. This can be attributed to the fact that in the old model, neglecting the reflection (including total reflection) at the surface and the collection efficiency by the lens (i.e., Eq. (6)) leads to over-prediction.

Figure 5 shows a set of normalized intensity profiles to compare the shape of the transmission profile. It shows the intensity profile of the transmitted photons at the

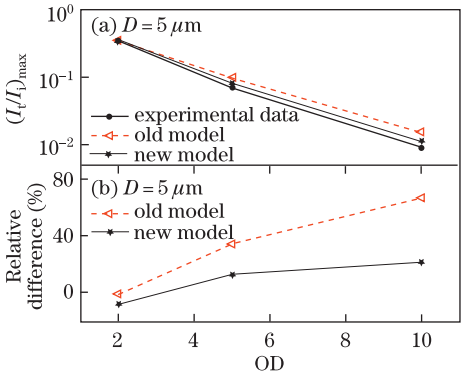

Fig. 4. (a) Summary of the peak transmission predicted by the old and new models compared with that obtained experimentally and (b) difference in the peak transmission of the old and new models relative to the experimental measurements. The acceptance angle is 8.5°.

mid-plane (i.e., along the z axis when y=0). The results were again compared with those obtained from the old model and the experimental measurements. All profiles were normalized to facilitate the comparison of the shape. As shown in Fig. 5, there is a noticeable difference in the intensity profiles between the old and the new models. With D=5 μm particles at OD=10, the FWHM predicted by the old and the new models differs by ~5% (3.43 mm versus 3.27 mm). The experimentally measured FWHM was 3.19 mm in this case[6]. Therefore, both the old and the new models over-predicted the FWHM, by ~7.5% and ~2.5% relative to the experimental measurements, respectively. The comparisons were also made under other conditions, and the results are summarized in Fig. 6. Figure 6(a) of shows the simulated FWHM of the intensity profile at the exit plane in comparison to the experimental measurements, while Fig. 6(b) shows the difference of the simulated FWHM relative to the experimental measurements. The new model predicts a FWHM that is different from that by the old model by an appreciable amount, which shows improved agreement with the experimental results. The cause of such difference in FWHM is more complicated than the intensity discussed above. Several factors (in addition to the generic scattering properties of the particles) considered in the new model affect the width of the transmitted profile: refraction, reflection, and lens collection. Refraction tends to increase the width of the transmitted profile, while both reflection and lens

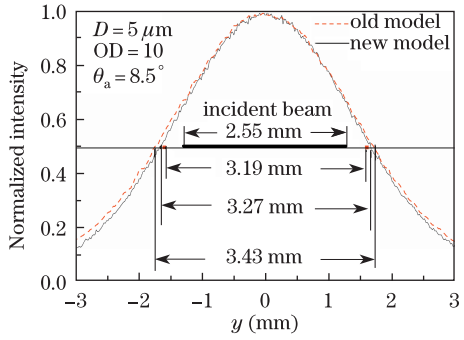

Fig. 5. Normalized intensity profile obtained using the new model in comparison to the results obtained from the old model and the experiments.

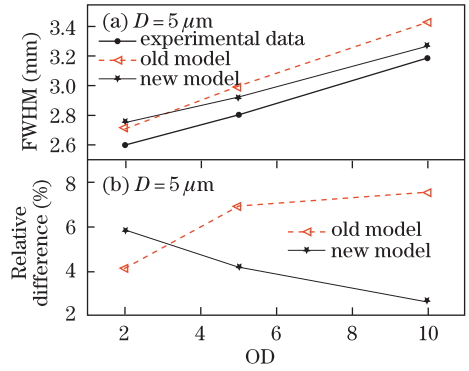

Fig. 6. (a) Summary of the FWHM predicted by the old and new models compared with that obtained experimentally and (b) difference in the FWHM of the old and new models relative to the experimental measurements. The acceptance angle is 8.5°.

collection tend to decrease the width of the transmitted profile. In this study, the transmitted photons exit from water (with higher refraction index) into air (with lower refraction index), hence refraction essentially bends the transmitted photons away from the forward direction and broadens the profile. On the other hand, reflection and lens collection tend to decrease the width of the transmitted profile because of the following: 1) a higher fraction of photons exiting at large angles are reflected according to Eq. (6); 2) total reflection completely blocked photons with angles larger than β_c from exiting; 3) the consideration of the lens collection according to Eq. (7) prevents photons exiting with large angles from being collected. These factors compete with each other, and the overall effects on FWHM vary with OD, as shown in Fig. 6.

In conclusion, a new model has been developed to integrate the MC method and geometrical optics for the simulation of multiple scattering. The model considers factors that have been usually neglected in past studies: refraction, reflection, and lens collection. This study has shown that the consideration of these factors from simple geometrical optics affects both the magnitude and shape of the profiles of the transmitted photons and generally improves the agreement with experimental measurements. Such improved agreement naturally motivates an integration of the MC model with a full-scale ray-tracing program[19] to simulate imaging using multiple scattered photons. Moreover, the model developed in this study offers several key advantages, such as the simplicity of implementation and the efficiency in execution. These are especially important when the model is applied to solve the inverse scattering problem.

We thank the authors of Ref. 6 (Drs. Berrocal, Sedarsky, Paciaroni, Meglinski, and Linne) for providing the laser source profile shown in Fig. 2 and for the many useful discussions.

References

1. J. C. Hebden, D. J. Hall, M. Firbank, and D. T. Delpy, Appl. Opt. **34,** 8038 (1995).
2. R. M. Measures, Laser Remote Sensing: Fundamentals and Applications (Krieger Publishing Company, Malabar, 1992).
3. M. A. Linne, M. Paciaroni, J. R. Gord, and T. R. Meyer, Appl. Opt. **44,** 6627 (2005).
4. A. A. Kokhanovsky, Meas. Sci. Technol. **13,** 233 (2002).
5. A. Ishimaru, *Electromagnetic Wave Propagation, Radiation, and Scattering* (Prentice Hall, Englewood Cliffs, NJ, 1991).
6. E. Berrocal, D. L. Sedarsky, M. E. Paciaroni, I. V. Meglinski, and M. A. Linne, Opt. Express **15,** 10649 (2007).
7. E. Berrocal, D. L. Sedarsky, M. E. Paciaroni, I. V. Meglinski, and M. A. Linne, Opt. Express **17,** 13792 (2009).
8. I. M. Sobol, *The Monte Carlo Method* (The University of Chicago Press, Chicago, 1967).
9. N. G. Chen, Appl. Opt. **46,** 1597 (2007).
10. H. O. D. Rocco, D. I. Iriarte, J. A. Pomarico, and H. F. Ranea-Sandoval, J. Quant. Spectrosc. Radiat. Transfer **110,** 307 (2009).
11. J. C. Ramella-Roman, S. A. Prahl, and S. L. Jacques, Opt. Express **13,** 10392 (2005).
12. J. C. Ramella-Roman, S. A. Prahl, and S. L. Jacques, Opt. Express **13,** 4420 (2005).
13. C. Calba, L. Mees, C. Roze, and T. Girasole, J. Opt. Soc. Am. **25,** 1541 (2008).
14. D. Contini, F. Martelli, and G. Zaccanti, Appl. Opt. **36,** 4587 (1997).
15. L. H. Wang, S. L. Jacques, and L. Q. Zheng, Comput. Meth. Prog. Bio. **47,** 131 (1995).
16. J. Ripoll and V. Ntziachristos, Mod. Phys. Lett. B **18,** 1403 (2004).
17. C. F. Bohren and D. R. Huffman, *Absorption and Scattering of Light by Small Particles* (Wiley-Interscience, New York, 1983).
18. E. Berrocal, "Multiple scattering of light in optical diagnostics of dense sprays and other complex turbid media", PhD. Thesis (Cranfield University, 2006).
19. D. Sedarsky, E. Berrocal, and M. Linne, Opt. Express **19,** 1866 (2011).